



## Bullion mixtures in silver coinage from ancient Greece and Egypt

Francis Albarede<sup>a,\*</sup>, Gillan Davis<sup>b</sup>, Liesel Gentelli<sup>a</sup>, Janne Blichert-Toft<sup>a</sup>, Haim Gitler<sup>c</sup>,  
Marine Pinto<sup>a</sup>, Philippe Telouk<sup>a</sup>

<sup>a</sup> Ecole Normale Supérieure de Lyon, 69007, Lyon, France

<sup>b</sup> Australian Catholic University, National School of Arts, North Sydney, NSW, 2060, Australia

<sup>c</sup> Israel Museum, Jerusalem, Israel

### ARTICLE INFO

#### Keywords:

Pb isotopes  
Silver coinage  
Greece  
Mixing  
Recycling

### ABSTRACT

Was silver coinage minted from fresh metal newly extracted from the mine or was it from recycled silver deriving from older coins, silverware, or cult objects? The answer helps understand the provenance of coins and their circulation. Using Pb isotopes, the present work proposes a method to disentangle the sources of 368 silver-alloy coins from Athens, Corinth, Aegina, Thasos, Thrace, Macedonia, and Ptolemaic Egypt. We outline a new mixing model based on Principal Component Analysis and allowing for multiple steps of bullion recycling. The first component accounts for 94–99% (typically 97–99%) of the total variance, which indicates that the data form a well-defined alignment indicative of a nearly binary mixture between two source ores referred to as ‘end-members’. Isotopic evidence establishes the subordinate but pervasive practice of remelting. The strong skewness of the first principal component distribution shows that lead is dominated by the binary mixing of end-members. The geologically young end-member has high  $^{206}\text{Pb}/^{204}\text{Pb}$  and is best exemplified by Laurion ore used in Athenian coinage. With the possible exception of Ptolemaic samples, the second end-member attests to the persistence of a low- $^{206}\text{Pb}/^{204}\text{Pb}$ , geologically much older, end-member. In most cases, the distributions of a further two principal components are nearly symmetric and can be considered normal. If they represent ore sources, their very small contribution to the total variance qualifies them as ‘noise’ (caused by random isotopic fluctuations in the ores and analytical issues). We find that the Pb isotope ratios in the coinage issued by each minting authority are distributed as a power law. The slope of this distribution varies from one mint to another, with the steepest slopes (Corinth and Ptolemaic Egypt) indicating the predominance of freshly mined silver. The shallow slope of Macedonia demands a larger proportion of geologically old Pb. Silver supplied to the mint of Athens shifted from a mixture of high- and low- $^{206}\text{Pb}/^{204}\text{Pb}$  in the late 6th c. BCE to a predominance of unmixed high- $^{206}\text{Pb}/^{204}\text{Pb}$  ore from the mines of Laurion thereafter and fell back to a mixture with intermediate Pb isotope compositions in the second half of the 4th c. BCE. The limitation of the present study resides in the relatively small number of Pb isotope data for each mint, which, in most cases, prevents a statistically significant analysis of these data by periods. Nevertheless, the quasi-binary nature of most silver mixes stands out as a new and strong first-order, albeit somewhat counterintuitive, inference from the present data.

There is little historical evidence for how the mints of ancient Greek city-states (*poleis*), leagues (*koinonia*), and kingdoms obtained their supplies of silver for minting coins, especially when they lacked domestic natural resources. Was bullion minted fresh from the mine, or exported and only minted or turned into other silver products on demand, or simply hoarded by, for example, the Achaemenid kings? To what extent was silver recycled multiple times, especially by melting down older coinage and temple offerings and striking new coinage, as illustrated for example by the Coinage Decree of Athens and allied cities

(Melville-Jones, 2007). Refining (Van Alfen, 2004) and recycling of bullion were the ultimate mechanisms by which silver of different origins mixed, such as in the case of the Persians (Blichert-Toft et al., 2022; Olivier et al., 2017). Silver moved around the Mediterranean through the agency of Phoenician and Greek traders and mercenaries (Davis, 2012), and by payment of tribute (Thuc. 1.96.1–2; 2.13.3), booty (Plut. Cimon 9.4), ransom (Hdt. 5.74.3), and reparations (Thuc. 1.101.3). Attempts were made by imperial Athens to mandate use of Athenian coinage (*IG I<sup>3</sup>*, 1453) and to deal with the problem of foreign and

\* Corresponding author.

E-mail address: [albarede@ens-lyon.fr](mailto:albarede@ens-lyon.fr) (F. Albarede).

<https://doi.org/10.1016/j.jas.2023.105918>

Received 27 September 2023; Received in revised form 19 November 2023; Accepted 11 December 2023

Available online 23 December 2023

0305-4403/© 2024 The Authors. Published by Elsevier Ltd. This is an open access article under the CC BY license (<http://creativecommons.org/licenses/by/4.0/>).

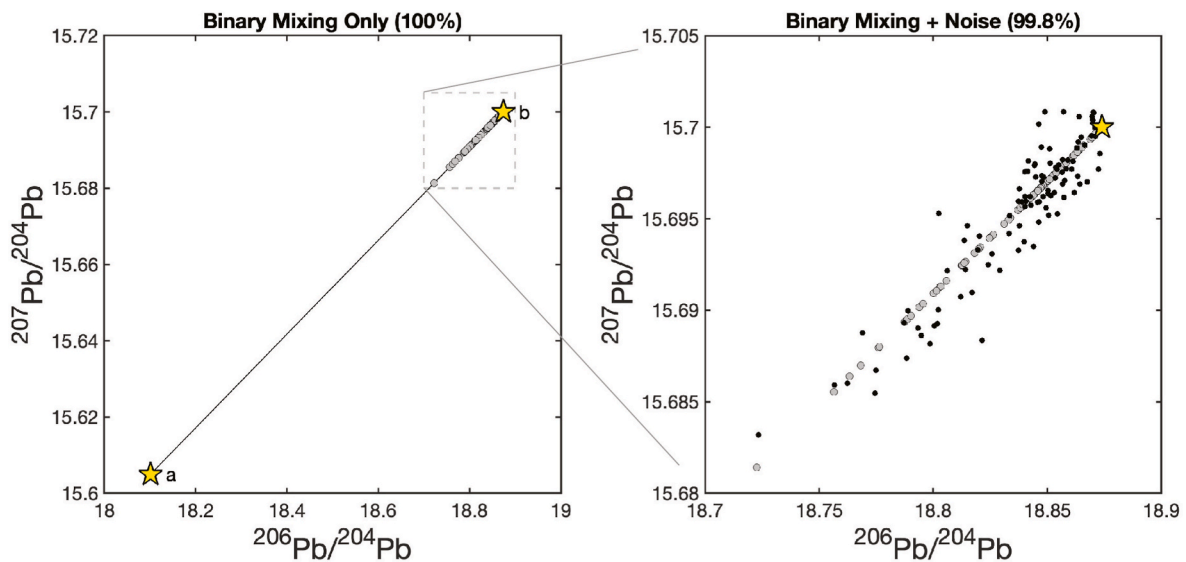


**Fig. 1.** Simulation of the respective effects of mixing and random noise on the  $^{206}\text{Pb}/^{204}\text{Pb}$  and  $^{207}\text{Pb}/^{204}\text{Pb}$  relationships for 100 coins. For clarity's sake, the example is represented in the 2-dimensional space of  $^{206}\text{Pb}/^{204}\text{Pb}$  and  $^{207}\text{Pb}/^{204}\text{Pb}$  values. The mixing proportions of end-members (=sources) a and b (yellow pentagrams) are strongly skewed towards the younger end-member b. The variability of Pb isotope compositions can be explained by the combination of variable proportions of end-members a and b (left) and random noise (right) introduced by natural and analytical variability. In the case of noise-free mixing (left), variance is explained at 100% by mixing by the first principal component (grey-filled symbols), whereas random noise (black symbols to the right) accounts for a small fraction (0.2%) of the variability. (For interpretation of the references to colour in this figure legend, the reader is referred to the Web version of this article.)

counterfeit coins being brought into the economy (Dem., 24.212–4, Stroud, 1974, 157–88). There is evidence of *poleis* and kingdoms requiring the use of their own coinage within their territory necessitating exchange for a small fee, though some major coinages, notably of Athens, would have had wide acceptance (Xen. *Poroi* 3.2; cf. discussion in Melville-Jones (2007), *SIG*<sup>3</sup>, 218 for Olbia; *P. Cairo Zen.* 59,021, 'The Revenue Papyrus of Ptolemy Philadelphus', Column 74 for Ptolemaic Egypt; Davis et al., 2020). Other than that, we are in the dark. Here we use the distribution of lead isotopes in silver coinages to address the question of the extent to which pure and mixed sources of silver were accessed by a selection of Greek, Macedonian, and Ptolemaic mints.

The geological association of lead and silver in ore matrices provides the justification for the use of Pb isotopes for sourcing the silver metal used for coinage and artifacts since lead was required to cupellate silver and traces of it remain in the final product. With the exception of Southern Iberia and a few other localities where argentiferous sulfates were formed by the weathering of sulfide seams, it is now clear that the major sources of silver were sulfidic ores, typically galena (PbS), and sulfosalts usually scattered throughout sulfidic ores (Chutas et al., 2008; Sack et al., 2002). This meant that non-local (exotic) Pb rarely needed to be added to cupellate the silver.

A major uncertainty overarches the focus of the present work. To what extent does a particular Pb isotope composition represent a specific mine district rather than a mixture created by remelting and/or restriking of coins and artifacts from different origins? To address this issue, we measured the Pb isotope compositions of 112 coins from Athens (ca. 525–290 BCE, including 19 *Wappenmünzen* and the rest being owls including 7 pi-style owls dating to 353–290 BCE), 56 from Corinthia (ca. 500–250 BCE, including 44 coins from Corinth and the rest from Sicyon and the *koinon* of Acarnania including Leucas), 18 from Aegina, and 38 from Thasos. More regional data are 50 coins from Thrace (east of the Strymon river but including Thasos), 48 from the kingdom of Macedonia (525–168 BCE), and 46 from Ptolemaic Egypt (Ptolemy I to Ptolemy XII) (Lorber, 2018, 2023). Among these, Aegina and Corinth were not primary silver producers but early major trading states relying on externally obtained sources to supply their mints (Gale et al., 1980). Egypt, tectonically restricted to the pan-African domain, also did not possess domestic silver ores (Price and Waggoner, 1975).

The Pb isotope data on coins show a broad scatter but with distinctive trends within the spread. Multiple potential factors account for Pb isotope variability: (1) The tectonic age of the ore, which is the time of separation of Pb from U and Th (radiogenic ingrowth); (2) the U/Pb and Th/U ratios of the source precursor; (3) mass-dependent isotope fractionation due to natural processes taking place at low temperature, such as weathering, hydrothermal activity, and Pb(II)/Pb(IV) equilibration between heterovalent oxidation states; and (4) mass-dependent isotope fractionation due to incomplete yields of Pb during purification by ion-exchange chromatography and erroneous correction of mass bias in the mass spectrometer during Pb isotope analysis. These problems have been reviewed elsewhere (Albarède et al., 2020).

An important aspect is the choice of isotope used to normalize Pb isotope ratios, most commonly  $^{206}\text{Pb}$  or  $^{204}\text{Pb}$ , because it provides different insights into the processes of interest. Normalization to  $^{206}\text{Pb}$  provides smooth arrays but only because radiogenic ingrowth and mass-dependent fractionation spread the data in the  $^{208}\text{Pb}/^{206}\text{Pb}$  vs  $^{207}\text{Pb}/^{206}\text{Pb}$  plot in nearly parallel directions, which lends to unresolvable ambiguity. Here, normalization to  $^{204}\text{Pb}$ , e.g., in the  $^{207}\text{Pb}/^{204}\text{Pb}$  vs  $^{206}\text{Pb}/^{204}\text{Pb}$  plot, was chosen because the angle between the two isotopic effects resulting from radiogenic ingrowth and mass-dependent fractionation, respectively, is now obtuse, and this optimizes information about which process controls the overall spread of the Pb isotopic data.

The problem of mixed sources of lead in archaeology was discussed by Stos-Gale (2001) who pointed out that binary mixtures in diagrams involving isotopic ratios should plot on the straight-line joining the points representing the masses of metal involved in the mixing. This important point should be corrected by the caveat that it is true *only* for isotopic ratios using the *same* normalization isotope. In particular, the statement fails for a plot such as  $^{208}\text{Pb}/^{204}\text{Pb}$  vs  $^{207}\text{Pb}/^{206}\text{Pb}$ , in which the mixing relationship is a hyperbola (Albarède, 1995; Albarède et al., 2021) and not a straight-line. The same confusion arises, as in Wood et al. (2017) when Pb isotopes are plotted as a function of any of the geochemically informed parameters, such as Pb model ages. For all these reasons, we restrict ourselves to  $^{204}\text{Pb}$ -normalized data.

Isotopic variability is due to two compounding factors: (1) mixing between end-members (not to be confused with principal components);

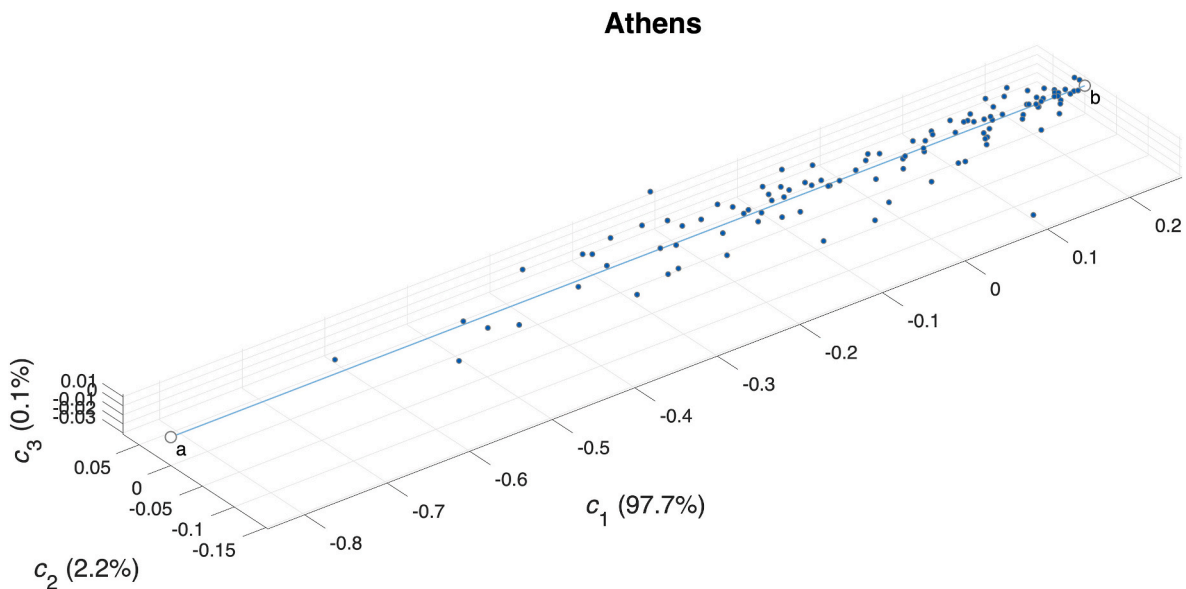


Fig. 2. PCA scores  $c_1$ ,  $c_2$ , and  $c_3$  of  $^{204}\text{Pb}$ -normalized isotope compositions for 112 Athenian silver coins (525–295 BCE). In spite of a long timespan of minting (see [https://www.youtube.com/watch?v=eLb5QKJs\\_14](https://www.youtube.com/watch?v=eLb5QKJs_14)), the data spread along the  $c_1$  axis and form a mixing line between bullion sources a and b. This axis explains 97.7% of the variance.

and, as mentioned above, (2) random noise due to mass fractionation in the ore, the chemistry lab, and the mass spectrometer plus intrinsic geochemical variability within the ore deposit itself (Fig. 1). For complex mixtures, Principal Component Analysis (PCA) is the method of choice (Baxter and Gale, 1998; also see a review of recent literature by Tomczyk and Żabiński, 2023). By an appropriate sequence of rotations in the original space of Pb isotope ratios, PCA reduces the number of dimensions in which large data sets are originally embedded to a new transformed representation that still contains most of the information contained in the original data set, but with a smaller number of dimensions.

In the absence of noise, the proportion of total variance explained by each principal component is key to the assessment of the number of metal sources.

- If 100% of the variance (variability) of the data is explained by *one* principal component, the data define a *straight-line* in both the original and transformed spaces. Mixing between two end-members manifests itself by a *straight-line passing through the end-members*. The straight-line indicates that the data set is accounted for by *two* different sources (*binary mixture* of two end-members). Large numbers of isotopically identical coins minted from pure ore seem unusual, which suggests that the workshop would normally take advantage of scrap silver accumulated in the mint. An example of end-members would be that a particular artifact could be formed by mixing silver from two distinct provenances (e.g., Laurion and Pangajon). Each projection will show linear relationships between the isotopic ratios.
- If *two* principal components are required to account for 100% of the variance, the data plot within a 3-dimensional *triangle* and *three* sources are required (*ternary mixture*). Binary plots will show scatter, except if the triangle is projected sideways: such a configuration explains the remarkable regularity of the widely used  $^{208}\text{Pb}/^{206}\text{Pb}$  vs  $^{207}\text{Pb}/^{206}\text{Pb}$  plots (Albarede et al., 2020).
- If the variance needs *three* principal components to be fully explained, no structure is discernible in the 3-dimensional space and *at least four* end-members are needed. No projection shows regularity.

The component scores (=loadings) of a particular sample are simply

its coordinates in the principal component representation. The breakdown into components is not a model or an assumption; it is a description of the mass conservation principle with the same certainty as death and taxes.

In the absence of mixing, noise manifests itself as a well-centered volley of buckshot. The combination of both mixing and noise produces scatter in isotopic plots. Fortunately, PCA can see through the combination of mixing and noise. When only two end-members can be seen, potential additional end-members are drowned in the noise and hence do not show up in the data. These additional end-members may be multiple, but evidence for their existence is missing.

Finally, it can be speculated that missing sources (end-members) have blended with each other to the extent that they appear to form a single component. Such mixtures would require a large number of melting/striking cycles for the original sources to escape disentanglement by PCA. In addition, such unnoticeable mixtures are expected to fall in an empty part of the isotopic space or, even worse, point to an apparent provenance for which evidence is faint or nonexistent.

### 1. The local statistical properties of Pb isotopes in silver coinage

The case of Athens well illustrates the geometry of the problem. Lead isotopes were determined for 112 silver coins dated from the Late Archaic period (*Wappenmünzen*, late 6th c. BCE) through to the Hellenistic period (early 3rd c. BCE). Discontinuities in the history of bullion supply and provenance, notably for coins minted from distinct masses of silver, can be handled in the multidimensional space of Pb isotope compositions. In order to assess the number of bullion sources and identify potential trends in the three-dimensional  $^{206}\text{Pb}/^{204}\text{Pb}$ – $^{207}\text{Pb}/^{204}\text{Pb}$ – $^{208}\text{Pb}/^{204}\text{Pb}$  space, we first determined the PCA scores [ $c_1$ ,  $c_2$ ,  $c_3$ ] of each datum from the data set considered. Given that isotopic ratios are of similar range, PCA can be calculated on the variance matrix after centering.

The first component scores along the first axis  $c_1$  typically account for 97–99% of the variance, which indicates that, in three-dimensional space, the variability of Pb isotopes is dominated by a linear array (Fig. 2) between two end-members a and b. The projection of the  $c_1$  values onto each plane of the three rectangular plots of the three ratios  $^{206}\text{Pb}/^{204}\text{Pb}$ ,  $^{207}\text{Pb}/^{204}\text{Pb}$ , and  $^{208}\text{Pb}/^{204}\text{Pb}$  defines an array which is oblique with respect to both of the trends of radiogenic ingrowth and

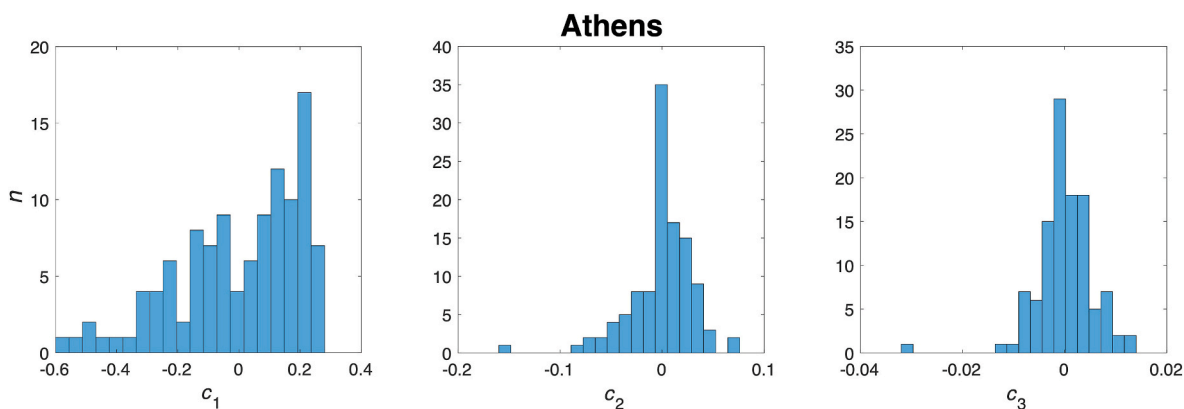


**Fig. 3.** Distribution of the three component scores obtained from PCA of Pb isotopic ratios measured in 112 Athenian silver coins. Note the skewed distribution of component  $c_1$ , which contrasts with the much more symmetric, nearly normal distribution of component  $c_3$ . Component  $c_2$  appears somewhat intermediate: although a hidden end-member may be present, this component does not account for enough variance (note horizontal scale) and the histogram is not different enough from a normal distribution for an additional end-member to be identified. The histogram skewness of  $c_1$  is strong evidence of mixing, whereas the more symmetric distributions of  $c_3$ , and to a large extent  $c_2$ , are suggestive of random noise.

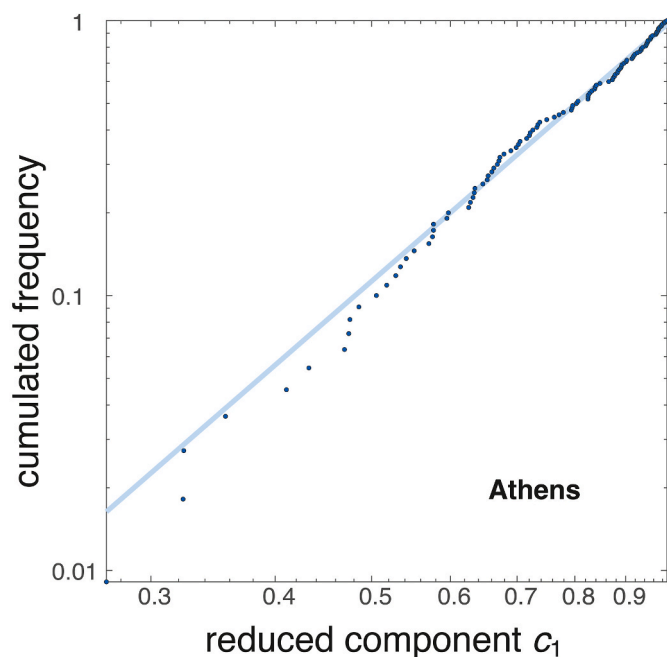


**Fig. 4.** Fit of the cumulated density function of the first reduced component  $r_1$  by a power law for 112 silver coins from Athens. The fit for >90% of the main population is excellent. The slope of the regression line is  $\alpha$ . The stronger noise around the straight-line at low values of  $c_1$  may result from variable proportions of other components with low- $^{206}\text{Pb}/^{204}\text{Pb}$  lead in a small number of coins (rogue samples).

mass-dependent fractionation. The distribution of component  $c_1$  is strongly skewed, which brings to mind that, in general, Pb isotopic data on ores and artifacts are not normally distributed (Baxter, 1999; Baxter and Gale, 1998). In contrast, the second component  $c_2$  and the very small component  $c_3$  are much more symmetrically distributed. The more symmetric aspect of the second component  $c_2$  and its small contribution to the variance (2.2%) prove that no more than two end-members are involved in the mixture.

The histograms of the smaller components  $c_2$  and  $c_3$  strongly suggest that they are dominated by random fluctuations and correspond to statistical noise. In contrast, the large asymmetric component  $c_1$  is definitely not consistent with a normal distribution and reflects mixing of two sources of silver with different Pb isotopic compositions sitting at

each end of the linear array. These are known as ‘end-members’. In other words, the trend stretching along the  $c_1$  axis is not controlled by random fluctuations but by the additive mixing of two contrasting masses of bullion with different Pb isotope compositions. The only accessible information on these end-members is that their  $c_1$  values must plot outside of the range defined by the Pb isotope data. Whether each end-member was added to the mixture in one or multiple steps, e.g., by successive (re) melting episodes, is what the new model is trying to address. Not only might these addition episodes have been multiple, they could also have occurred at different points in time, such as progressive enrichment of an old silver ‘mix’ by later addition of freshly mined silver.

The fraction of scores  $c_1$  is maximum next to the upper end-member  $b$  with score  $c_0^b$  and decreases exponentially away from it towards its lower end-member  $a$  with score  $c_0^a$  (Fig. 3). We used the standard optimization technique (see Appendix) provided by Matlab to determine the cumulative density function (cdf)  $F(r)$  of the reduced mixing variable  $r_1 = (c_1 - c_0^a)/(c_0^b - c_0^a)$  defined on  $[0,1]$  to adjust it to an exponential distribution. In a plot of  $\log F(r)$  vs  $\log r$  (Fig. 4), the data form a remarkable alignment corresponding to  $\text{cdf } F_{R_1}(r_1) = r_1^\alpha$  indicating that the scores  $c_1$  are distributed following a truncated power law with positive  $\alpha$  exponent between the upper and lower values  $c_0^a$  ( $r_1 = 0$ ) and  $c_0^b$  ( $r_1 = 1$ ) of the end-members. A more conventional power law with a negative  $\alpha$  exponent and defined over  $[0, \infty[$  is obtained by replacing the variable  $r_1$  by the variable  $r'_1 = (c_0^b - c_1)/(c_1 - c_0^a) = (1 - r_1)/r_1$ , although at the cost of not explicitly using mixing proportions  $r_1$ . Optimization by the Matlab numerical software returns the values of  $c_0^a$ ,  $c_0^b$ , and  $\alpha$  and their 95% confidence interval. The Pb isotope ratios corresponding to  $c_0^a$  and  $c_0^b$  are back-calculated from the principal components. For clarity, subscript 1 may hereinafter be omitted from symbols  $r$  and  $c$ .

## 2. The significance of the power law

To chemists and geochemists, the variable  $r$  brings mixing processes to mind: each sample represents a mixture of two metal fractions with Pb isotope compositions  $c_0^a$  and  $c_0^b$  (as determined by PCA and which can be back-calculated as true isotope ratios) or, equivalently, with reduced variable values  $r = r_a = 0$  and  $r = r_b = 1$ . The simple theory of mixing calculations applies indifferently to actual Pb isotopic ratios and to component scores.

Given the overwhelming predominance of the first component variance and the remarkably asymmetric distribution of its scores, mixing can be considered binary. Let us assume that each new issue is minted using fresh bullion extracted from the mine, here the mines of

Laurion, and recycled silver, which can be derived from either ‘rogue’ sources or a nondescript mix of multiple sources with low  $^{206}\text{Pb}/^{204}\text{Pb}$ . All the calculations are made on the isotopes of Pb contained in coinage. We will assume that the Pb proportion (caveat: not the mass of silver) of fresh silver (end-member b) in the mix at the first step is denoted by  $\varphi$  and the proportion of recycled Pb (a) is  $1-\varphi$ . The value  $c_1$  of the mix in the first issue is given by:

$$c_1 = (1 - \varphi)c_0^a + \varphi c_0^b \quad (1)$$

For simplicity we assume that from one issue to the next, the proportion  $\varphi$  does not change. The value  $c_2$  of the mix in the second issue is:

$$\begin{aligned} c_2 &= (1 - \varphi_2)[(1 - \varphi_1)c_0^a + \varphi_1 c_0^b] + \varphi_2 c_0^b \\ &= (1 - \varphi)^2 c_0^a + 2\varphi c_0^b - \varphi^2 c_0^b \end{aligned} \quad (2)$$

where it was assumed that  $\varphi_1 = \varphi_2 = \varphi$ . In addition, the contributions of antepenultimate and prior issues are neglected, which is equivalent to assuming that products of more than 2 terms in  $\varphi$  and  $1 - \varphi$  are small with respect to lower-degree terms. For the  $n$ -th issue, the equivalent equation therefore is:

$$c_n = (1 - \varphi)c_{n-1} + \varphi c_0^b \quad (3)$$

This is a difference equation which has the general solution:

$$\begin{aligned} c_n &= (1 - \varphi)^n c_0^a + \{1 - (1 - \varphi)^n\} c_0^b \\ &= c_0^b + (1 - \varphi)^n (c_0^a - c_0^b) \end{aligned} \quad (4)$$

or

$$\frac{c_0^b - c_n}{c_0^b - c_0^a} = 1 - r = (1 - \varphi)^n \quad (5)$$

which gives the dependence of the time-integrated mixing parameter  $r$  with respect to parameters  $\varphi$  and  $n$ . In order to estimate  $n$  from  $F_R(r)$ , let us now use the observation that the reduced, time-integrated mixing variable is distributed as a power-law cdf with exponent  $\alpha$ :

$$F_R(r) = r^\alpha \quad (6)$$

which is equivalent to the following point density (or frequency) function  $f_R(r)$  (pdf):

$$f_R(r) = \frac{dF_R(r)}{dr} = \alpha r^{\alpha-1} \quad (7)$$

The pdf of the mixing parameter  $\varphi$  is:

$$\begin{aligned} f_{\varphi,n}(\varphi) &= f_R[r(\varphi)] \left| \frac{dr}{d\varphi} \right| \\ &= \alpha n (1 - \varphi)^{n-1} [1 - (1 - \varphi)^{n\alpha}]^{\alpha-1} \\ &= d[1 - (1 - \varphi)^{n\alpha}] / d\varphi \end{aligned} \quad (8)$$

which gives the following expression for the cdf:

$$F_{\varphi,n}(\varphi) = [1 - (1 - \varphi)^{n\alpha}] \quad (9)$$

consistent with Eqns (5) and (6). The assumption of negligible contributions from the earliest issues could be relieved in a numerical code, but at the expense of the clarity of the deep model structure and for little benefit.

The parameter  $\alpha$  is the exponent of the power law distribution of the time-integrated proportion  $r$  of end-member b in the coinage of a given polis. The parameter  $\varphi$  is the proportion of end-member b in the coinage at each minting cycle. Different numbers  $n$  of mixing/recycling loops are consistent with a same value of the parameter  $\alpha$ . Note that  $F_{\varphi,1}(\varphi) = F_R(r)$ .

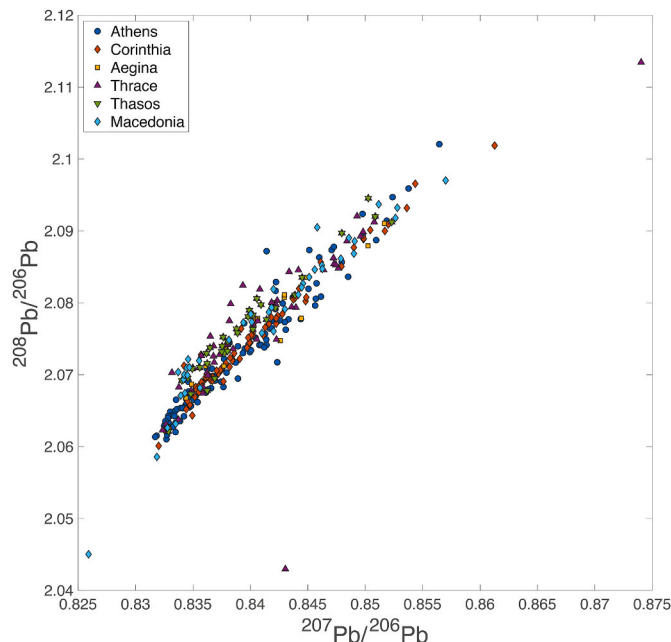


Fig. 5. Conventional plot of  $^{208}\text{Pb}/^{206}\text{Pb}$  vs  $^{207}\text{Pb}/^{206}\text{Pb}$  for six of the seven data sets considered in this work. In order to preserve readability, Ptolemaic coinage has not been included. Note that Thasos samples also appear in the Thrace data set.

### 3. Results

The calculation used for Athenian silver coins was extended to other data sets: Corinthia, Aegina, Thasos, Thrace (east of the Strymon river), Macedonia, and Ptolemaic Egypt. The data are provided as an Excel spreadsheet in the Supplemental Table T1. A conventional plot of  $^{208}\text{Pb}/^{206}\text{Pb}$  as a function of  $^{207}\text{Pb}/^{206}\text{Pb}$  is presented in Fig. 5 without the data on Ptolemaic coinage so as to preserve readability. The size of the files containing the coin photographs (2.8 Gb) exceeds the limit allowed by the journal but they can be requested from the authors and will be uploaded to a public database. These photographs are for the purpose of identification only.

In general, the alignments are excellent at high values of  $c_1$  with increasing scatter at low values. The Pb isotope compositions of the high- $^{206}\text{Pb}/^{204}\text{Pb}$  end-members b form a rather tight group with Cenozoic (<65 Ma) apparent ages, typically Laurion and the Cyclades (Stos-Gale et al., 1996; Vaxevanopoulos et al., 2022), whereas the spread of the low- $^{206}\text{Pb}/^{204}\text{Pb}$  end-members a is significantly larger and reflects Late Proterozoic to Late Paleozoic sources (~700–250 Ma), typically the Rhodopes, the Balkans, Sardinia, and the Sierra Morena (Vaxevanopoulos et al., 2022; Westner et al., 2023).

### 4. Discussion and concluding remarks

Inferences on provenances drawn from the Pb isotope compositions of end-members a and b are laid out and discussed in Albarede et al. (2024). Here we focus on mixing only.

The strong isotopic evidence of mixing establishes the pervasive practice of remelting and the less frequent restriking without melting such as is the case with the Athenian pi-style owls called in and restruck in the wake of the Social War (357–355 BCE) (Bingen, 1969; de Callatay, 2018; Flament, 2007; Kroll, 2011). The present results show that restriking without remelting is a minor occurrence in the Greek numismatic record.

The relatively small number of analyses obtained for each mint forced us, unfortunately, to consider the data over long periods. This limitation should not be minimized, but, as an upside, the number of

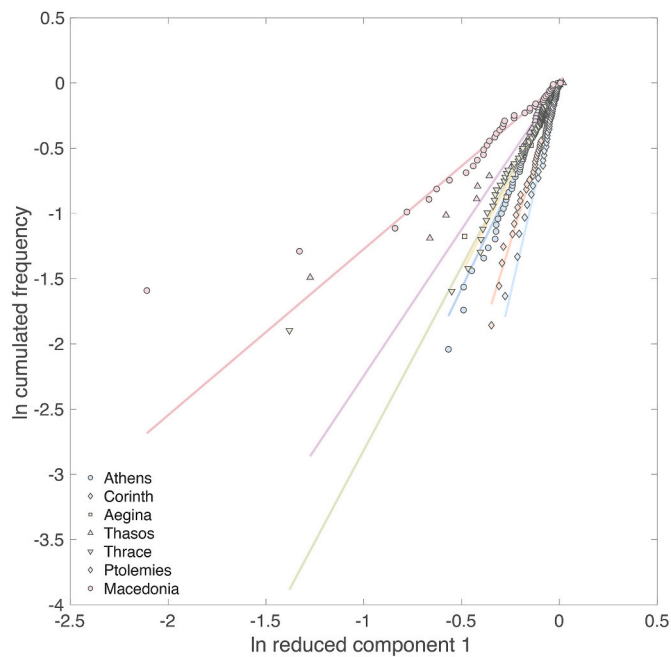


**Fig. 6.** Log-log plot of the cumulated density function  $F_R(r)$  for all the data sets. Their strong linearity is suggestive of the binary character of source mixing.

bullion sources identified by PCA is shown to be limited to two in most cases. The sources of bullion used by the various mints remained relatively stable over time. The data set of Fig. S3 nevertheless suggests that their relative contribution changed through time.

When two end-members account for most of the isotopic variability, additional end-members are drowned within the noise and do not manifest themselves in the data. The linearity of the cumulative density function in a log-log plot (Fig. 4) of the isotopic variations in the coinage of a particular *polis* or kingdom confirms the dominantly binary mixing and that the sources of bullion remained almost unchanged over the centuries, even if, as in the case of Athens where the mines of Laurion dominated the supply from the 5th to the beginning of the 3rd c. BCE, the relative proportions contributed by each end-member may have changed with time (Fig. S3).

The model reflects the power-law distribution of the first component score  $c_1$ : the Pb isotope compositions of most coins are close to the value of the geologically young, high- $^{206}\text{Pb}/^{204}\text{Pb}$  dominating end-member while the contribution of the geologically older, low- $^{206}\text{Pb}/^{204}\text{Pb}$  end-member is small. This explains that, even though some samples with a larger fraction of the geologically old end-member may misdirect the search, the Pb isotopes of most coins will still reveal, although with some noise, the provenance of the young silver component.

The steeper the slope  $\alpha$ , the steeper the histogram of the first component  $c_1$  (Fig. 6). Steep slopes, such as those observed for Corinth and Egypt, reveal the dominance of the geologically young, high- $^{206}\text{Pb}/^{204}\text{Pb}$  silver component in their silver coinage. Trade between Corinth and Athens, but also wider exchanges involving multiple partners, may have funneled high- $^{206}\text{Pb}/^{204}\text{Pb}$  bullion from Laurion into the mints of *poleis* lacking silver mines. The observation is similar for Ptolemaic Egypt. Multiple minting loops acting to rapidly recycle Athenian silver coinage may create the false impression that Laurion-like silver production was much larger than broad estimates suggest. The presence of Laurion-like silver and high  $\alpha$  values confirm that money minted in Athens was widely used for foreign trade. In contrast, the low  $\alpha$  value observed in Macedonian coinage appears to reflect a larger proportion of the geologically old, low- $^{206}\text{Pb}/^{204}\text{Pb}$  in its silver.

Smaller proportions of variance accounted for by the first component are compensated by larger proportions inferred for the second

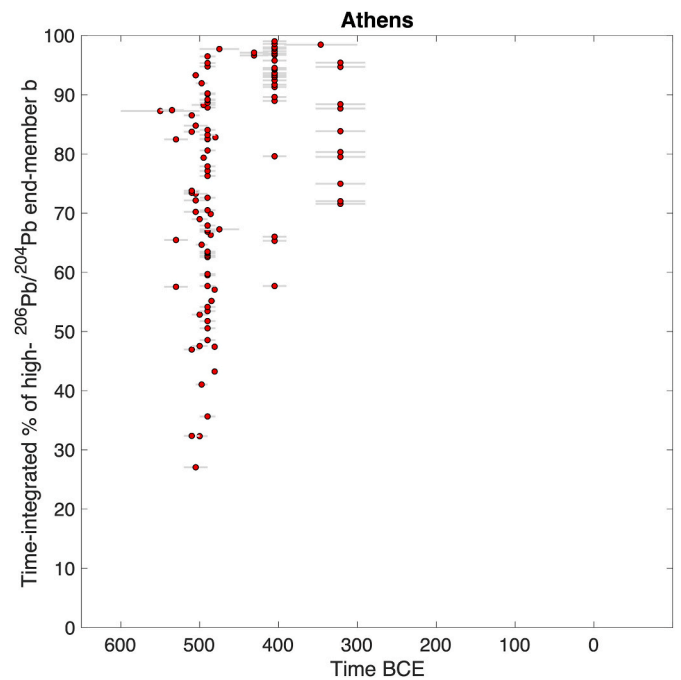


**Fig. 7.** Variation of the time-integrated proportion  $r$  of end-member  $b$  (high  $^{206}\text{Pb}/^{204}\text{Pb}$ , presumably from Laurion) in principal component 1 (97.7% of the variance) in 112 Athenian silver coins as a function of time of minting. Horizontal bars indicate the range of minting dates associated with each coin. The *Wappenmünzen* (early coinage from the late 6th c. BCE) contain a prominent fraction of low- $^{206}\text{Pb}/^{204}\text{Pb}$  bullion from Macedonia and Thrace. This fraction is definitely smaller in Classical coins (5th c. BCE), which reflects the large productivity of high- $^{206}\text{Pb}/^{204}\text{Pb}$  silver from the Laurion mines or the rapid recycling of earlier productions. The latest issues show no strong grouping and reflect multiply recycled Pb.

component. This is the case with the coinages of Thrace and the Ptolemies. The larger spread in the plane  $c_2$  vs  $c_1$  may indicate the presence of one or more additional recycled sources of bullion.

A major shift in Athenian silver supply is clearly visible when the proportion of high- $^{206}\text{Pb}/^{204}\text{Pb}$  bullion is plotted as a function of the age of minting (Fig. 7). The contrast is particularly strong between the early coinage of the *Wappenmünzen* and the subsequent owls: the former contains a range of different sources and includes low- $^{206}\text{Pb}/^{204}\text{Pb}$  bullion, whereas the latter is dominated by high- $^{206}\text{Pb}/^{204}\text{Pb}$  values consistent with a Laurion source. In contrast, the late issues show a relatively uniform distribution, which may indicate that recycling prevailed at the time of Macedonian conquest.

Evidence of recycling and mixing is a straightforward consequence of the simple theory laid out above. Let us assume a value of  $\alpha = 3$  and use Eqn (8) with  $n = 1 \dots 8$  recycling stages (Fig. 8). The peak of  $\varphi$  moves, as expected, towards lower time-integrated  $r$  values as  $n$  increases, but finally converge to a stable value. In other words, some data sets reflect a smaller contribution of low- $^{206}\text{Pb}/^{204}\text{Pb}$  silver input and higher proportions of recycled material. This is the most likely explanation for the lower time-integrated  $r$  values in the late 4th c. BCE issues of Athenian coinage. The Athenian mint started out with a large proportion of bullion with low  $^{206}\text{Pb}/^{204}\text{Pb}$  values, *i.e.* non-Laurion sources possibly from Thrace (+Troas) and Macedonia as demonstrated in Albarede et al. (2024). By the start of the Classical period, the high- $^{206}\text{Pb}/^{204}\text{Pb}$  Laurion silver became the dominant source of bullion (>90%). Subsequently, coinage minted in the second part of the 4th c. BCE is largely dominated by multiply recycled silver. This coincides with a period during which the production of Athenian tetradrachms seems to have dwindled (Kroll, 2011). Nevertheless, Kroll (2011) offers a new reading of Xenophon's 355 BCE discussion of the Athenian economy. The production of the

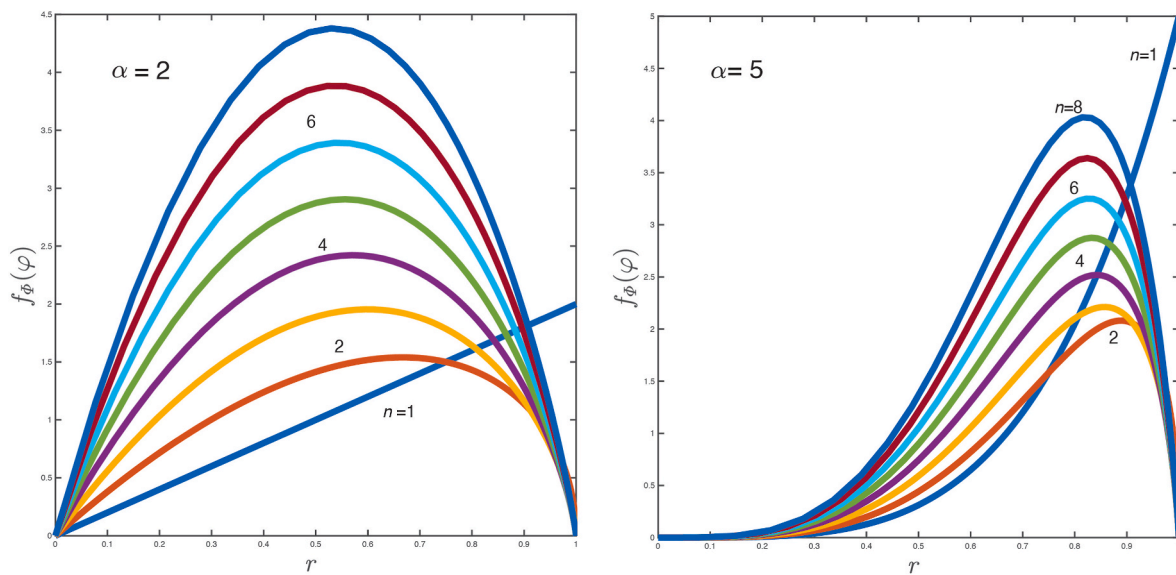


**Fig. 8.** Different numbers  $n$  of recycling steps are consistent with a same value of the slope  $\alpha$ . Point density function (pdf) of the mixing variable  $\varphi$  for successive recycling steps ( $n = 1 \dots 8$ ) as a function of the reduced mixing variable  $r = (c_1 - c_0^a)/(c_0^b - c_0^a)$ . Note the larger proportion of the low- $^{206}\text{Pb}/^{204}\text{Pb}$  end-member for  $\alpha = 2$  with respect to the case  $\alpha = 5$ . The maximum of  $f_\varphi(\varphi)$  moves from  $r = 1$  for the first issue and converge towards smaller values when  $n$  increases. Slope values of  $\alpha = 2$  and  $\alpha = 5$  are assumed. Multiply recycled silver shows that most coins appear to contain 80–90% recycled lead.

**Table 1**

Calculation output.  $n$  is the number of silver coins in each data set. Columns 3–5 list  $\alpha$  values and their 95% confidence limits. The scores  $c_1$  of the first PCA component are distributed following a power law between the upper  $c_0^a$  ( $r = 0$ ) (recycled bullion) and lower  $c_0^b$  ( $r = 1$ ) (silver from the most productive mines, such as those of Laurion) end-member values. The Pb isotope compositions listed in the last six columns correspond to those of the end-members a and b  $c_0^a$  and  $c_0^b$ .

Set	$n$	$\alpha$	$\alpha (-)$	$\alpha (+)$	$c_a$	$c_b$	$^{206}\text{Pb}/^{204}\text{Pb}_a$	$^{207}\text{Pb}/^{204}\text{Pb}_a$	$^{208}\text{Pb}/^{204}\text{Pb}_a$	$^{206}\text{Pb}/^{204}\text{Pb}_b$	$^{207}\text{Pb}/^{204}\text{Pb}_b$	$^{208}\text{Pb}/^{204}\text{Pb}_b$
Athens	112	3.15	3.09	3.21	-0.845	0.263	18.101	15.605	38.135	18.874	15.700	38.923
Corinthia	56	4.88	4.74	5.02	-1.139	0.235	17.855	15.581	37.863	18.803	15.683	38.852
Aegina	18	2.91	2.57	3.26	-0.708	0.223	18.165	15.589	38.115	18.755	15.676	38.830
Thasos	38	2.24	2.01	2.48	-0.403	0.186	18.379	15.646	38.464	18.793	15.679	38.882
Thrace	50	2.81	2.72	2.91	-0.712	0.265	18.215	15.624	38.146	18.800	15.683	38.926
Macedonia	48	1.27	1.20	1.34	-0.464	0.356	18.308	15.630	38.358	18.870	15.691	38.951
Ptolemies	46	6.46	6.22	6.71	-0.996	0.159	18.027	15.593	37.954	18.748	15.675	38.852

Laurion mines may have dried up because entrepreneurs had become averse to the financial risks associated with opening new mines (Xen. *Poroi* 4.28), but Xenophon (Xen. *Poroi* 4.7) also warns that ‘if a man finds himself with a huge amount of it, he takes as much pleasure in burying the surplus as in using it’, i.e., hoarding silver by weight becomes an attractive financial alternative to minting.

In the Corinthia coins, an influx of fresh, low- $^{206}\text{Pb}/^{204}\text{Pb}$  bullion only becomes apparent in the mid-4th c. BCE both from the high  $\alpha$  value and the evolution of mixing with minting age (Table 1, Figs. S2 and S3).

The significance of the  $r$  and  $\varphi$  values should not be mistaken: these variables refer to proportions of Pb from the different sources, not to proportions of silver. In Davis (2012), Pb contents are distributed as a log-normal variable with a geometric mean of 0.22 (0.03–1.8 wt%) at the 95% confidence level. We nevertheless suggest that the bullion fractions of Pb inferred from isotopes echo similar trends for silver.

#### Declaration of competing interest

None.

#### Acknowledgements

This work is a contribution of Advanced Grant 741454-SILVER-ERC-2016-ADG ‘Silver Isotopes and the Rise of Money’ awarded to FA by the European Research Council. François de Callatay has been of great help with result interpretation. We thank François de Callatay and Johan van

Heesch for granting access to the numismatic collection of the Royal Library of Brussels. George Kakavas allowed access to the collection of the Numismatic Museum of Athens. Elena Kontou and her group are thanked for help during sampling. We also acknowledge with thanks access to the collections of the Israel Museum in Jerusalem. We thank two anonymous reviewers and Editor Marcos Martín-Torres for very useful comments.

#### Appendix A. Supplementary data

Supplementary data to this article can be found online at <https://doi.org/10.1016/j.jas.2023.105918>.

#### References

- Albarede, F., 1995. *Introduction to Geochemical Modeling*. Cambridge University Press, Cambridge.
- Albarede, F., Blichert-Toft, J., Gentelli, L., Milot, J., Vaxevanopoulos, M., Klein, S., Westner, K., Birch, T., Davis, G., de Callatay, F., 2020. A miner’s perspective on Pb isotope provenances in the Western and Central Mediterranean. *J. Archaeol. Sci.* 121, 105194.
- Albarede, F., Blichert-Toft, J., de Callatay, F., Davis, G., Debernardi, P., Gentelli, L., Gitler, H., Kemmers, F., Klein, S., Malod-Dognin, C., 2021. From commodity to money: the rise of silver coinage around the Ancient Mediterranean (sixth–first centuries BCE). *Archaeometry* 63, 142–155.
- Albarede, F., Davis, G., Blichert-Toft, J., Gentelli, L., Gitler, H., Pinto, M., Telouk, P., 2024. A new algorithm for using Pb isotopes to determine the provenance of bullion used for ancient Greek coinage. *J. Archaeol. Sci.*

- Baxter, M., 1999. On the multivariate normality of data arising from lead isotope fields. *J. Archaeol. Sci.* 26, 117–124.
- Baxter, M.J., Gale, N.H., 1998. Testing for multivariate normality via univariate tests: a case study using lead isotope ratio data. *J. Appl. Stat.* 25, 671–683.
- Bingen, J., 1969. Le trésor monétaire. *Thorikos* 6, 7–59.
- Blichert-Toft, J., de Callatay, F., Tèlouk, P., Albarède, F., 2022. Origin and fate of the greatest accumulation of silver in ancient history. *Archaeological and Anthropological Sciences* 14, 1–10.
- Chutas, N.I., Kress, V.C., Ghiorso, M.S., Sack, R.O., 2008. A solution model for high-temperature PbS-AgSbS<sub>2</sub>-AgBiS<sub>2</sub> galena. *Am. Mineral.* 93, 1630–1640.
- Davis, G., 2012. Dating the drachmas in Solon's laws. *Historia* 61, 127–158.
- Davis, G., Gore, D.B., Sheedy, K.A., Albarède, F., 2020. Separating silver sources of Archaic Athenian coinage by comprehensive compositional analyses. *J. Archaeol. Sci.* 114, 105068.
- de Callatay, F., 2018. Overstriking in the Greek world: an overview on the full landscape and an explanation for punctual occurrences with silver coinage. *Rev. Belge Numismatique Sigillogr.* 24–57.
- Flament, C., 2007. L'argent des chouettes: bilan de l'application des méthodes de laboratoire au monnayage athénien tirant parti de nouvelles analyses réalisées au moyen de la méthode PIXE. *Rev. Belge Numismatique Sigillogr.* 9–30.
- Gale, N.H., Gentner, W., Wagner, G.A., 1980. Mineralogical and geographical sources of archaic Greek coinage. In: Metcalf, D.M., Oddy, W.A. (Eds.), *Metallurgy in Numismatics*, vol 1, London.
- Kroll, J.H., 2011. The reminting of Athenian silver coinage, 353 BC: for George Cawkwell in his 91st year. *Hesperia. The Journal of the American School of Classical Studies at Athens* 80, 229–259.
- Lorber, C.C., 2018. Coins of the Ptolemaic Empire. In: Part 1: Ptolemy I through Ptolemy IV, vol. 1. *Precious Metal*, American Numismatic Society, New York.
- Lorber, C.C., 2023. Coins of the ptolemaic empire. Part 2: Ptolemy V through cleopatra VII. In: *Precious-Metal Catalogue and Plates*, umé 2. American Numismatic Society, New York.
- Melville-Jones, J., 2007. *Testimonia Numaria Volume II*. Spink Books, London.
- Olivier, J., Duyrat, F., Carrier, C., Blet-Lemarquand, M., 2017. Minted Silver in the Empire of Alexander, Alexander the Great, a Linked Open World. Ausonius Éditions, pp. 127–146.
- Price, M., Waggoner, N., 1975. *Archaic Greek Coinage: the Asyut Hoard*. VC Vecchi, London.
- Sack, R.O., Kuehner, S.M., Hardy, L.S., 2002. Retrograde Ag-enrichment in fahlroes from the Coeur d'Alene mining district, Idaho, USA. *Mineral. Mag.* 66, 215–229.
- Stos-Gale, Z.A., Gale, N.H., Annetts, N., 1996. Lead isotope data from the Isotrace Laboratory, Oxford: archaeometry data base 3, ores from the Aegean, part 1. *Archaeometry* 38, 381–390.
- Stos-Gale, Z.A., 2001. The impact of natural sciences on studies of hacksiber and early silver coinage. In: Balmuth, M.S. (Ed.), *Hacksilber to Coinage: New Insights into the Monetary History of the Near East and Greece*. Amer. Num. Soc., New York, pp. 53–76.
- Stroud, R.S., 1974. An Athenian Law on Silver Coinage. *Hesperia* 43, 157–188.
- Tomczyk, C., Żabiński, G., 2023. A PCA-AHC approach to provenance studies of non-ferrous metals with combined Pb isotope and chemistry data. *J. Archaeol. Method Theor.*
- Van Alfen, P.G., 2004. Herodotus' "aryandic" silver and bullion use in Persian-period Egypt. *Am. J. Numismatics* 7–46, 1989.
- Vaxevanopoulos, M., Blichert-Toft, J., Davis, G., Albarède, F., 2022. New findings of ancient Greek silver sources. *J. Archaeol. Sci.* 137, 105474.
- Westner, K.J., Vaxevanopoulos, M., Blichert-Toft, J., Davis, G., Albarède, F., 2023. Isotope and trace element compositions of silver-bearing ores in the Balkans as possible metal sources in antiquity. *J. Archaeol. Sci.* 155, 105791.
- Wood, J.R., Charlton, M.F., Murillo-Barroso, M., Martínón-Torres, M., 2017. Iridium to provenance ancient silver. *J. Archaeol. Sci.* 81, 1–12.